Sensitivity of tree species performance to climate and competition changes across their range distribution

Willian Vieira*[1], Andrew MacDonald[1], and Dominique Gravel[1]

[1]Département de biologie, Université de Sherbrooke, Sherbrooke, QC, Canada

Running title: Tree sensitivity to climate and competition

Supporting information: Additional supporting information can be found here.

Acknowledgments: We thank nice people

Data availability: All the code and data used to reproduce the analysis, figure and manuscript are stored as a research compendium at https://github.com/willvieira/ms_forest-ipm-sensitivity).

Funding: This research was supported by the BIOS² NSERC CREATE program.

Conflicts of interest: The authors declare no conflict of interest.

Abstract

Demographic range models, designed to scale individual variation to predict population growth rate, offer a more mechanistic approach to assessing species distribution than

*Corresponding author: willian.vieira@usherbrooke.ca

phenomenological models. Despite numerous forest models adopting this approach to explore the influence of climate and competition on species population growth rate, the correlation of species performance with their distribution is often weak. What remains unclear is whether the mismatch between species performance and distribution arises from modelling limitations or if climate and competition are poor predictors of species distribution. Here, we developed an Integral Projection Model to evaluate the impact of climate and competition on all demographic components of 31 tree species from eastern North America. By using flexible nonlinear hierarchical models, we filled most of the gaps in previous studies while accounting for process uncertainty. Using perturbation analysis, we found that population growth rate was more sensitive to mean annual temperature than conspecific and heterospecific competition for all species. Furthermore, we examined how population growth rate sensitivity to climate and competition varied across the species range. The dominance of climate over competition increased as species approached the cold or hot temperature ranges. Moreover, most species exhibited a decline in population growth rate sensitivity to competition from the cold to the hot temperature range. Notably, the most influential variable remained the local plot conditions captured by the random effects. Unveiling species-specific sensitivity to climate and competition provides crucial insights into how species may respond to emerging conditions resulting from climate change and disturbance changes.

Keywords: Integral Projection Models, Perturbation analysis, demography performance

1 Introduction

The urge to unravel species distribution processes has increased with the current global crisis, where 15 to 37% of species are expected to face extinction due to climate change (Thomas et al. 2004). This urgency is particularly pertinent for long-lived sessile species like trees, whose range distribution is likely to fail to follow climate change (Zhu et al. 2012, Sittaro et al. 2017). In an effort to enhance traditional correlative species distribution models (e.g. Guisan and Zimmermann 2000), theory decomposes species distribution into smaller components to develop a more mechanistic, process-based approach (Evans et al. 2016). One

such approach is demographic range models, which predicts a species' distribution based on individual performance determined by growth, survival, and recruitment rates (Pagel and Schurr 2012). This approach operates under the hypothesis that population growth rate (λ), determined by demographic rates, varies across the environment, with the species range limit defined by conditions where λ is positive (Maguire Jr 1973, Holt 2009). By approaching species distribution from a demographic perspective, we can account for the complexity of forest dynamics arising from multiple features such as environment and species interaction (Schurr2012; Svenning et al. 2014).

Several studies have attempted to predict species distribution based on demographic performance of forest trees. The most basic version of these models uses environment-dependent demographic rates to predict λ (e.g. Merow et al. 2014, Csergő et al. 2017). However, factors like competition undeniably influence both demographic rates (Clark et al. 2011, Luo and Chen 2011, Zhang et al. 2015) and population performance (Scherrer et al. 2020, Le Squin et al. 2021) in forest trees. This realized version of the niche (Hutchinson 1957) may explain why North American forest trees often do not occur within their climatically suitable range (Boucher-Lalonde et al. 2012, Talluto et al. 2017).

An increasing body of evidence conflicts with theoretical expectations by observing weak correlations between the demographic performance of trees and their distribution (McGill 2012, Csergő et al. 2017, Bohner and Diez 2020, Le Squin et al. 2021, Midolo et al. 2021, Guyennon et al. 2023, Thuiller et al. 2014). This mismatch is often attributed to the oversight of processes beyond climate and competition. For instance, habitat availability coupled with dispersal limitations can restrict a species' distribution even in locations where performance is positive (Pulliam 2000). However, the precision of methods used to quantify demographic performance is rarely challenged, perhaps in part because each attempt employs a different approach. Some studies assess performance based solely on one of the growth, survival, or recruitment rates (McGill 2012, Bohner and Diez 2020). When demographic rates are integrated into population models, specific components, such as recruitment, are often overlooked due to data limitations (Kunstler et al. 2021, Le Squin et al. 2021). Moreover, some studies do not account for density dependence (Csergő et al. 2017, Ohse et al. 2023), and when they do, they rarely differentiate between conspecific and heterospecific competition (Bohner and Diez 2020, Le Squin et al. 2021). Finally, despite the need to embrace model and data uncertainty (Milner-Gulland and Shea 2017), most of these studies assessed performance under average covariate conditions and pointwise estimations,

neglecting the associated uncertainty of the estimates.

Rather than asking whether demographic performance correlates with distribution, a more fruitful question may be how climate and competition influence demographic performance. Indeed, we still miss a comprehensive partitioning of the sensitivity of forest dynamics to local and biogeographical drivers of performance (Ohse et al. 2023). For instance, Clark et al. (2011) found that annual growth rate is more sensitive to competition, while fecundity is more sensitive to climate. In contrast, Copenhaver-Parry and Cannon (2016) found that growth was more sensitive to climate than competition. These studies provide crucial insights into how forest trees will respond to climate change and forest management, supporting conservation planning. However, they only assess the importance of climate and competition on single demographic components, lacking a complete picture of population dynamics. This is especially critical if species are susceptible to variation in sensitivity to climate and competition across life history stages (Russell et al. 2012, Ettinger and HilleRisLambers 2013). Furthermore, the sensitivity of λ to climate and competition may depend on the species range position, such as climate being relatively more important in abiotic stressful conditions and competition being more critical when climate is benign (Louthan et al. 2015). Nevertheless, such information is still lacking for trees (Ohse et al. 2023).

Here, we evaluate how climate and competition affect the demography and population growth rate of the 31 most abundant forest tree species across Eastern North America. We leverage the complete (26 - 53°) latitudinal coverage of forest inventories across the US and Canada to capture the entire range of these species. Specifically, we model each of the growth, survival, and recruitment vital rates as a function of mean annual temperature and precipitation, as well as conspecific and heterospecific basal area density, serving as a proxy for competition for light. We fit these demographic models with a flexible, non-linear hierarchical Bayesian model. The non-linear approach captures both the complexity of trees' demographic rates and the multiple-effect forms of climate and competition. Furhtermore, the hierarchical Bayesian approach allows one to account for model uncertainty at different organizational scales. These demographic rate models are then incorporated into a size-structured Integral Projection Model (IPM) to quantify the λ of each species under climate and competition effects.

Our primary goal is to use the fitted IPM to compute the sensitivity of each species' λ to climate and competition across their range. Employing perturbation analysis, we quantify the relative contribution

of each covariate to changes in λ (Caswell 2000). Precisely, we assess the species sensitivity of an observed λ for each plot-year combination based on their specific climate and competition conditions. This approach enables an evaluation of the overall sensitivity of λ to a covariate while considering the inherent variability of the covariate experienced by the species. For instance, a species may exhibit high sensitivity to temperature, but if most of its distribution is observed under optimal temperature conditions, the average sensitivity of the species will be low.

Lastly, expanding on previours findings indicating the inability of North American trees to both expand their cold range and contract their hot range under climate change (Talluto et al. 2017), we ask if sensitivity to climate and competition changes across the species' cold and hot ranges. Furthermore, we explore whether the relative sensitivity between climate and competition changes across the species' distribution range. Our integrative approach allows us to assess the relative effects of climate and competition from demographic rates up to the population growth rate while accounting for model uncertainties and stand structure, revealing essential insights into understanding the response of forest trees to climate change, management practices, and conservation efforts.

2 Methods

2.1 Forest inventory and climate data

We used two open inventory datasets from eastern North America: the Forest Inventory and Analysis (FIA) dataset in the United States (O'Connell et al. 2007) and the Forest Inventory of Québec (Ministère des Ressources Naturelles 2016). At the plot level, we focused on plots sampled at least twice, excluding those that had undergone harvesting to concentrate solely on natural dynamics. Specifically, we selected surveys conducted for the FIA dataset using the modern standardized methodology implemented since 1999. After applying these filters, our final dataset encompassed nearly 26,000 plots spanning a latitude range from 26° to 53° (Figure S7). Each plot within the dataset was measured between 1970 and 2021, with observation frequencies ranging from 2 to 7 times and an average of 3 measurements per plot. The time intervals between measurements varied from 1 to 40 years, with a median interval of 7 years (Figure S7).

These datasets provide individual-level information on the diameter at breast height (DBH) and the status (dead or alive) of more than 200 species. From this pool, we selected the 31 most abundant species (Table S1). This selection comprises 9 conifer species and 22 hardwood species. We ensured an even distribution of species across the shade tolerance axis, with three species classified as very intolerant, nine as intolerant, eight as intermediate, eight as tolerant, and five as very tolerant (Burns et al. 1990).

For the competition metric, we use asymmetric competition for light, meaning that each individual is affected only by neighbour individuals of larger size. We quantified asymmetric competition for light for a focal individual in a given plot by summing the total basal area of all individuals larger than the focal one, herein BAL. We further split BAL into the total density of conspecific and heterospecific individuals. For the climate variable, we obtained the 19 bioclimatic variables with a 10 km^2 (300 arcsec) resolution grid, covering the period from 1970 to 2018. These climate variables were modeled using the ANUSPLIN interpolation method (McKenney et al. 2011). We used each plot's latitude and longitude coordinates to extract the mean annual temperature (MAT) and mean annual precipitation (MAP). In cases where plots did not fall within a valid pixel of the climate variable grid, we interpolated the climate condition using the eight neighboring cells. Due to the transitional nature of the dataset, we considered both the average and standard deviation of MAT and MAP over the years within each time interval.

2.2 Model

We evaluated the population growth rates of the 31 forest species using an Integral Projection Model (IPM). An IPM is a mathematical tool used to represent the dynamics of structured populations and communities. It distinguishes itself from traditional population models with the representation of a continuous trait in discrete time (Easterling et al. 2000). This is especially relevant for trees due to the considerable variability in demographic rates depending on individual size (Kohyama 1992). Specifically, the IPM consists of a set of functions predicting the transition of a distribution of individual traits from time t to time $t + 1$:

$$n(z', t+1) = \int_L^U K(z', z, \theta)\, n(z, t)\, \mathrm{d}z \tag{1}$$

The continuous trait z at time t represents the DBH, bouded between the lower (L) and upper (U) values, and $n(z,t)$ characterizes the continuous DBH distribution for a population. The probability of the population distribution size from $n(z,t)$ to $n(z', t+1)$ is governed by the kernel K and the species-specific parameters θ. The kernel K, a continuous version of the discretized projection Matrix in structured population models, is composed of three sub-models:

$$K(z', z, \theta) = [Growth(z', z, \theta) \times Survival(z, \theta)] + Recruitment(z, \theta) \tag{2}$$

The growth function describes how individual trees increase in size, while the survival function determines the probability of staying alive throughout the next time step. The recruitment model describes the number of individuals ingressing the population. Below, we describe the basic (intercept) version of these models, followed by the inclusion of each climate and competition covariate.

2.2.1 Demographic rates

Growth - the size in DBH of an individual at time $t + \Delta t$ after growing from time t is determined by:

$$dbh_{i,t+\Delta t} \sim N(\mu_{i,t+\Delta t}, \sigma) \tag{3}$$

We used the von Bertalanffy growth equation to describe the annual growth rate in DBH of an individual i (Von Bertalanffy 1957). The average size at time $t + \Delta t$ from the initial size $dbh_{i,t}$ of an individual at time t is given by:

$$\mu_{i,t+\Delta t} = dbh_{i,t} \times e^{-\Gamma \Delta t} + \zeta_\infty (1 - e^{-\Gamma \Delta t}) \tag{4}$$

Where Δt is the time interval between the initial and final size measurements and Γ represents a

dimensionless growth rate coefficient. ζ_∞ denotes the asymptotic size, which is the location at which growth approximates to zero. The rationale behind this model is that the growth rate exponentially decreases with size, converging to zero as size approaches ζ_∞. This assumption is particularly valuable in the context of the IPM, as it prevents eviction — where individuals are projected beyond the limits of the size distribution ($[L, U]$) defined by the Kernel.

Survival - The chance of a mortality event (M) for an individual i within the time interval between t and $t + \Delta t$ is modeled as a Bernoulli distribution:

$$M_i \sim Bernoulli(p_i) \tag{5}$$

Here, M_i represents the individual's status (alive/dead) and p_i the mortality probability of the individual i. The mortality probability is calculated based on the annual survival rate (ψ) and the time interval between census (Δt):

$$p_i = 1 - \psi^{\Delta t} \tag{6}$$

The model assumes that the survival probability $(1 - p_i)$ increases with the longevity parameter ψ, but is compensated exponentially with the increase in time Δt.

Recruitment - We combined data from the U.S. and Quebec forest inventories to obtain a broader range of climatic conditions. However, these inventories have inconsistent protocols for recording seedlings, saplings, and juveniles. Most of all, they have different size thresholds for individual-based measurements. Therefore, we quantified the recruitment rate (I) as the ingrowth of new individuals into the adult population, defined as those with a DBH exceeding 12.7 cm. The quantity I encompasses the processes of fecundity, dispersal, growth, and survival up to reaching the size threshold. Similar to growth and survival, the count of ingrowth individuals (I) reaching the 12.7 cm size threshold depends on the time interval between measurements. We introduce two parameters to control the potential number of recruited individuals: ϕ, determining the annual ingrowth rate per square meter, and ρ, denoting the annual survival probability of each ingrowth individual:

$$I \sim Poisson(\ \phi \times A \times \frac{1-\rho^{\Delta t}}{1-\rho}\ ) \tag{7}$$

Where A represents the area of the plot in square meters. The model assumes that new individuals enter the population annually at a rate of ϕ, and their likelihood of surviving until the subsequent measurement (ρ) declines over time. Note that ρ in Equation 7 is not associated with Equation 6 determining the survival of the adults. Instead, ρ is estimated from the data of individuals arriving in the population. Once an individual is recruited into the population, a submodel determines its initial size z_I, increasing linearly with time:

$$z_I \sim TNormal(\Omega + \beta\Delta t,\ \sigma,\ \alpha,\ \beta) \tag{8}$$

The $TNormal$ is a truncated distribution with lower and upper limits determined by the α and β parameters, respectively. We set α to 12.7 cm, aligning it with the ingrowth threshold, while β is set to infinity to allow for an unbounded upper limit.

2.2.2 Covariates

Random effects - We introduced plot-level random effects in each of the growth, survival, and recruitment demographic component to account for shared variance between the individuals within the same plot. For a demographic component with an average intercept $\overline{I}$, an offset value (α) is drawn for each plot j from a normal distribution with a mean of zero and variance σ:

$$\begin{aligned} \alpha_j &\sim N(0, \sigma) \\ I_j &= \overline{I} + \alpha_j \end{aligned} \tag{9}$$

Where σ represents the variance among all plots j and I can take one of three forms: Γ for growth, ψ for survival, and ϕ for the recruitment model.

Competition - We used basal area of larger individuals (BAL; asymmetric competition) instead of total basal area (BA; symmetric competition), assuming that competition for light is the primary competitive factor driving forest dynamics (Pacala et al. 1996). Therefore, each of the growth (Γ), longevity (ψ), and recruitment survival (ρ) parameters decreases exponentially with BAL. Take I as one of the three parameters, the effect of BAL on I is driven by two parameters describing the conspecific (β) and heterospecific (θ) competition:

$$I + \beta(BAL_{cons} + \theta \times BAL_{het}) \tag{10}$$

When $\theta < 1$, conspecific competition is stronger than heterospecific competition. Conversely, heterospecific competition prevails when $\theta > 1$, and when $\theta = 1$, there is no distinction between conspecific and heterospecific competition. Note that β is also unbounded, allowing it to converge towards negative (indicating competition) or positive (indicating facilitation) values. Furthermore, we fixed $\theta = 1$ for the recruitment ($I = \rho$) due to model convergence issues. The recruitment model also accounts for the conspecific density dependence effect on the annual ingrowth rate (ϕ). Specifically, ϕ increases with BAL_{cons} as a positive effect of seed source up to reach the optimal density of recruitment, δ, where it then decreases with more conspecific density due to competition at a rate proportional to σ:

$$\phi + \left(\frac{BAL_{cons} - \delta}{\sigma}\right)^2 \tag{11}$$

Climate - We selected mean annual temperature (MAT) and mean annual precipitation (MAP) bioclimatic variables as they are widely used in species distribution modeling and were previously found relevant to model demography of these species (Le Squin et al. 2021). Each demographic component I, representing either Γ for growth, ψ for longevity, or ϕ for ingrowth, varies as a bell-shaped curve determined by an optimal climate condition (ξ) and a climate breadth parameter (σ):

$$I + \left(\frac{MAT - \xi_{MAT}}{\sigma_{MAT}}\right)^2 + \left(\frac{MAP - \xi_{MAP}}{\sigma_{MAP}}\right)^2 \tag{12}$$

The climate breadth parameter (σ) influences the strength of the specific climate variable's effect on each demographic component. This unimodal function is flexible, assuming various shapes, such as bell, quasi-linear, or flat shapes. However, this flexibility introduces the possibility of parameter degeneracy or redundancy, where different combinations of parameter values yield similar outcomes. To address this issue, we constrained the optimal climate condition parameter (ξ) within the observed climate range for the species, assuming that the optimal climate condition falls within our observed data range.

2.2.3 Model fit and validation

We fitted each of the growth, survival, and recruitment models separately for each species, using the Hamiltonian Monte Carlo (HMC) algorithm implemented in the Stan software (version 2.30.1 Team and Others 2022) with the `cmdstandr` R package interface (version 0.5.3 Gabry et al. 2023). We conducted 2000 iterations for the warm-up and 2000 iterations for the sampling phase for each of the four chains, resulting in 8000 posterior samples (excluding the warm-up). However, we kept only the last 1000 iterations of the sampling phase to save computation time and storage space, resulting in 4000 posterior samples. We build and fit each demographic component incrementally, from a simple intercept, and gradually incorporate plot random effects, competition, and climate covariates. Recall that our goal is not to have the most complex model to achieve the highest predictive metric but to make inferences (Tredennick et al. 2021). We focus on assessing the relative effects of climate and competition while controlling for other influential factors. Therefore, our modeling approach is guided by biological mechanisms, which tend to provide more robust extrapolation (Briscoe et al. 2019) rather than being solely dictated by specific statistical metrics. Nevertheless, we checked if increasing model complexity with new covariates does not result in worse performance using complementary metrics such as mean squared error (MSE), pseudo R^2 (Gelman et al. 2019), and Leave-One-Out Cross-Validation (LOO-CV). Detailed discussions regarding model fit, diagnostics, and model comparison can be found in supplementary material 1.

With the fitted demographic components, we constructed the Kernel K of the IPM following Equation 2. We employed the mid-point rule to perform the discrete-form integration of the continuous K (Ellner et al. 2016). This involved discretizing the projection kernel K using bins of 0.1 cm, which are considered appropriate for obtaining unbiased estimates (Zuidema et al. 2010). Finally, we computed

the asymptotic population growth rate (λ) using the leading eigenvalue of the discretized matrix K.

2.3 Perturbation analysis

We use perturbation analysis to assess the sensitivity of λ to competition and climate conditions (Caswell 2000). We define sensitivity as the partial derivative of λ with respect to a covariate X, which can take the form of either conspecific or heterospecific density dependence competition, or temperature or precipitation climate conditions. In practice, we quantify sensitivity by slightly increasing each covariate value X_j to $X_j^{'}$ and computing the change in λ following the right-hand part of Equation 13:

$$\left.\frac{\partial \lambda_{ij}}{\partial X_j}\right|_{K_{ij}} \approx \frac{\Delta \lambda_{ij}}{\Delta X_j} = \frac{|f(X_j^{'}) - f(X_j)|}{X_j^{'} - X_j} \tag{13}$$

Sensitivity is evaluated separately for each species i and is conditional on the specific climate and competition conditions observed for the plot j, along with the Kernel K_{ij} parameters. We set the perturbation size to a 1% increase in the normalized scale for each covariate. For instance, a 1% increase translates to a rise of 0.3°C for Mean Annual Temperature (MAT) and 26 mm for Mean Annual Precipitation (MAP). Because the competition metric is computed at the individual level, the perturbation was applied to each individual, where a 1% increase corresponds approximately to a rise of 1.2 cm in dbh. As we were interested in the absolute difference, the resulting sensitivity value ranges between 0 and infinity, with lower values indicating a lower sensitivity of λ to the specific covariate. We computed the log ratio between competition and climate (CCR) sensitivities to discern their relative effects as follows:

$$\begin{aligned} S_{comp,ij} &= \frac{\partial \lambda_{ij}}{\partial BA_{cons,i}} + \frac{\partial \lambda_{ij}}{\partial BA_{het,i}} \\ S_{clim,ij} &= \frac{\partial \lambda_{ij}}{\partial MAT_i} + \frac{\partial \lambda_{ij}}{\partial MAP_i} \\ CCR_{ij} &= \ln \frac{S_{comp,ij}}{S_{clim,ij}} \end{aligned} \tag{14}$$

Here, S represents the total sensitivity of species i to competition or climate for a given plot j. Negative

CCR values indicate higher sensitivity of λ to climate, while positive values indicate the opposite.

When averaging $S_{X,i}$ across j, this metric reflects the sensitivity of λ_i to X, which is conditional upon the probability distribution of the covariate X. We categorized each plot into cold, center, or hot conditions along the MAT axis for every species. Plots were labeled as cold (or hot) if the average MAT fell below (above) the 10% (90%) probability distribution, with all intermediate plots considered center plots. Thus, sensitivity to a covariate in the cold range of the species signifies the average sensitivity among all plots classified as cold. It is important to note that this classification is also conditional on the probability distribution of observed MAT within the species.

The code to fit each demographic component is available in the `TreesDemography` GitHub repository. The code for the IPM model and the respective sensitivity analysis is available in the `forest-IPM` GitHub repository.

3 Results

3.1 Model validation

All species-specific demographic components demonstrated convergence with $\hat{R} < 1.05$ and low to no divergent iterations. In comparing the simple intercept model with the more complete versions, the LOO-CV consistently favored the complete model for all three demographic rates, featuring plot random effects, competition, and climate covariates, over other competing models (supplementary material 1). The absolute values of LOO-CV suggested that the growth model gained the most information from including covariates, followed by recruitment and survival models. We further validated our model predictions by comparing the parameters with traits groups such as growth rate classes, maximum observed size, maximum observed age, shade tolerance, and seed mass (Burns et al. 1990, Díaz et al. 2022).

The growth model intercept comprises two parameters, one determining the asymptotic size (ζ_∞) and the annual growth rate Γ. The ζ_∞ can be interpreted as the maximum predicted size of the species, which correlates well across all 31 species with the maximum observed size in the literature ($R^2 = 0.31$, Figure 1). Similarly, Γ among the species exhibited a distribution aligning with the fast, moderate,

and slow-growing traits (Figure S8). In the survival model, the expected longevity (L) can be derived from the annual survival rate (ψ) following the equality $L = e^{\psi}$, showing a high correlation with the maximum observed age in the literature ($R^2 = 0.59$, Figure 1). In the recruitment model, the log of the annual ingrowth rate (ϕ) reduced linearly with seed mass (Figure S9), capturing the seed mass-growth rate tradeoff (Reich et al. 1998). Additionally, the annual survival probability of ingrowth (ρ) decreased with intolerance to shade (Figure S10).

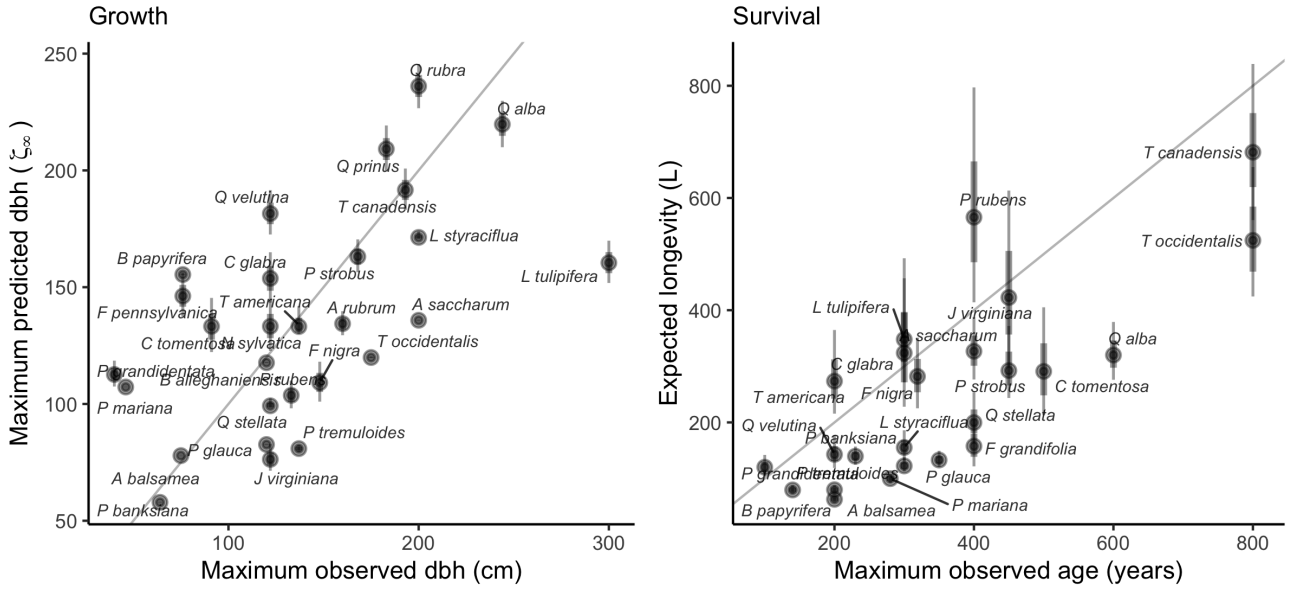

Figure 1: Correlation between predicted asymptotic size (ζ_∞) with maximum observed size (left) and predicted longevity (L) with maximum observed age for the 31 forest species. Maximum observed size and age are obtained from Burns et al. (1990). The gray line is the identity curve.

Both conspecific and heterospecific competition effects for the growth and survival models increased with intolerance to shade (Figure 2). The stronger competition effect of conspecific over heterospecific was consistent for almost all species in both growth and survival models. Only two species for growth and three for survival among the 31 presented stronger heterospecific competition than conspecific competition. Moreover, *Fagus grandifolia* and *Thuja occidentalis* exhibited positive density dependence for the survival model. For recruitment, the effect of total stand density increased with shade intolerance among the species (Figure S11).

The distribution of optimal MAT (ξ_{MAT}) and MAP (ξ_{MAP}) for the 31 species revealed that the optimal climates for growth, survival, and recruitment were rarely located at the center of the species ranges (Figure S12 and S13). Furthermore, most species exhibited some degree of demographic compensation,

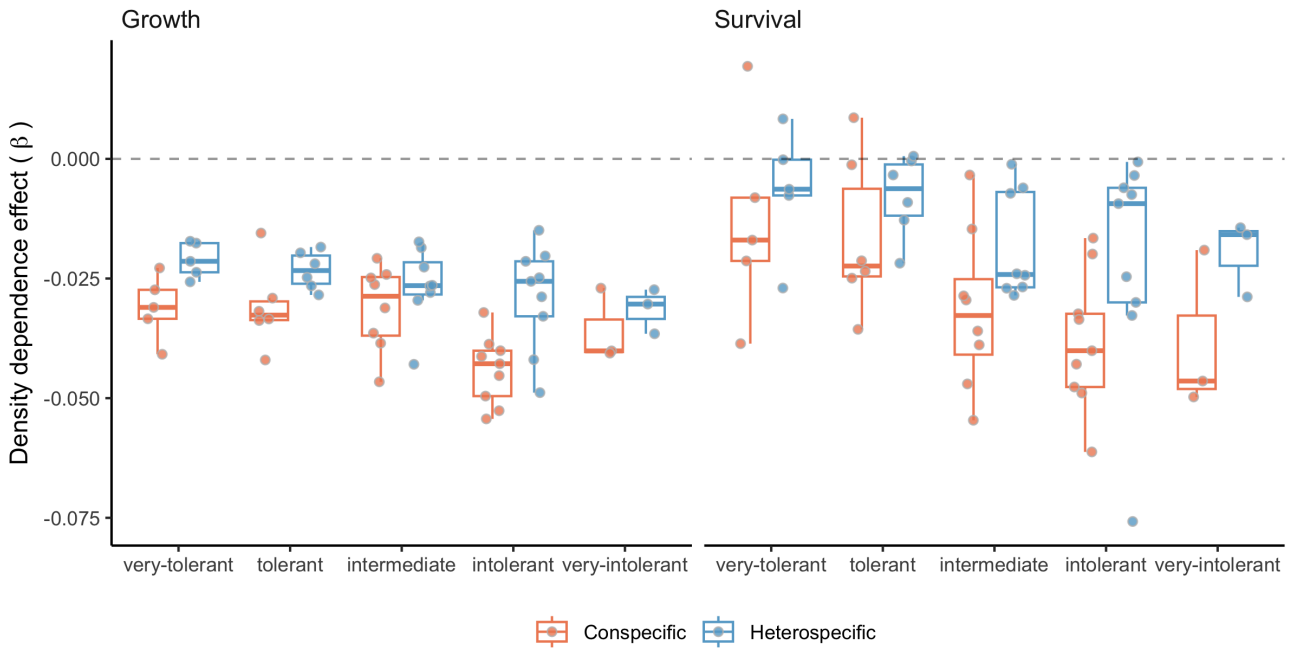

Figure 2: Posterior distribution for the conspecific (red) and heterospecific (blue) density dependence for each class of shade tolerance (Burns et al. 1990). The more negative the β, the stronger the competition effect.

that is, opposing responses to the environment between demographic rates (Villellas et al. 2015). Lastly, the climate breadth (σ) determined how flat or narrow the performance of species was across MAT and MAP. We found among all species that climate breadth increased with range size, demonstrating that species with more range occupancy had larger niche breadths. The exception was the niche breadth of survival over MAT, showing a weak, flat correlation.

3.2 λ sensitivity to climate and competition

We used perturbation analysis to assess the relative contribution of each covariate to changes in λ. Figure 3 describes the average sensitivity of each species' population growth rate to conspecific and heterospecific competition, temperature, and precipitation. Across all species, λ exhibited higher sensitivity to temperature, followed by conspecific and heterospecific competition, while sensitivity to mean annual precipitation was practically zero. This observation of sensitivity to the covariates was consistent across all species.

We split plots into different regions to ask for each species if sensitivity to climate and competition

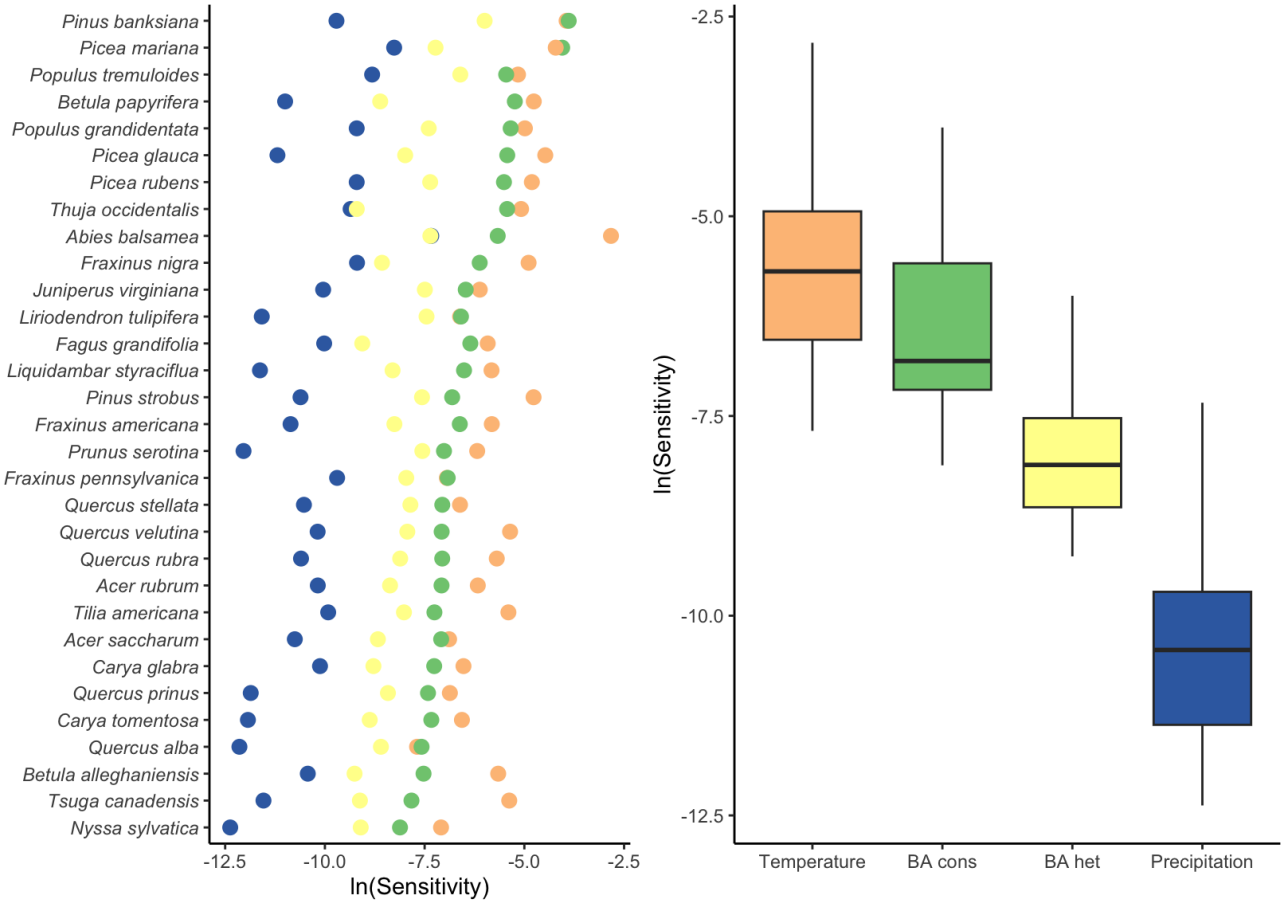

Figure 3: Log sensitivity of species population growth rate to conspecific competition, heterospecific competition, mean annual temperature, and mean annual precipitation across all plot-year observations. The smaller the values, the lower the sensitivity to a covariate.

changes between cold and hot portions of the range (Figure 4). We evaluate the sensitivity of each species' border location according to the average Mean Annual Temperature (MAT) among all plots of the species' border group. Species distributed toward colder temperature ranges often exhibited a decrease in sensitivity to climate from the cold to the hot border. Conversely, most species in the hot range distribution demonstrated increased sensitivity to climate at the hot border compared to the cold. Most species also presented a decreased sensitivity to competition from the cold to the hot border. The decrease in sensitivity to competition from the cold to the hot border was more pronounced for boreal species.

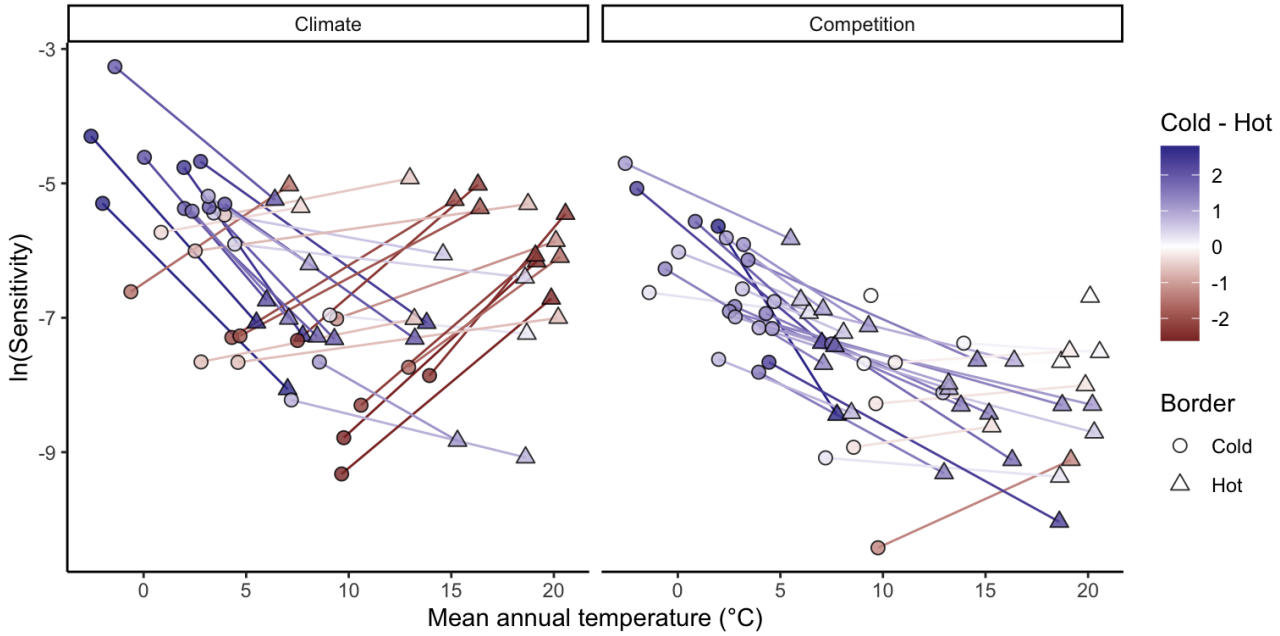

Figure 4: Differences in species population growth rate sensitivity to climate (left) and competition between the cold and hot range limits. Each species is represented by a connected line linking their cold (circle) and hot (triangle) range positions, colored according to the difference between the cold and hot sensitivities. Note that uncertainty in each sensitivity point estimation has been omitted for clarity.

We further explore the relative sensitivity between climate and competition changes across the species' range distribution (Figure 5). λ was more sensitive to climate than competition for almost all species across the cold, center, and hot ranges ($ln(CCR)$ below zero). Across the MAT range distribution, the relative effect of climate to competition increased toward both the cold and hot borders of the range. This indicates that species located at the extremes of the MAT range distribution are even more sensitive to climate than species at the center. Interestingly, the reason for this increase is not the

same for the cold and hot ranges. In the cold range, the sensitivity of λ increased for both climate and competition but was proportionally larger for climate. Conversely, in the hot range, the relative sensitivity to climate increased due to a significant decrease in sensitivity to competition.

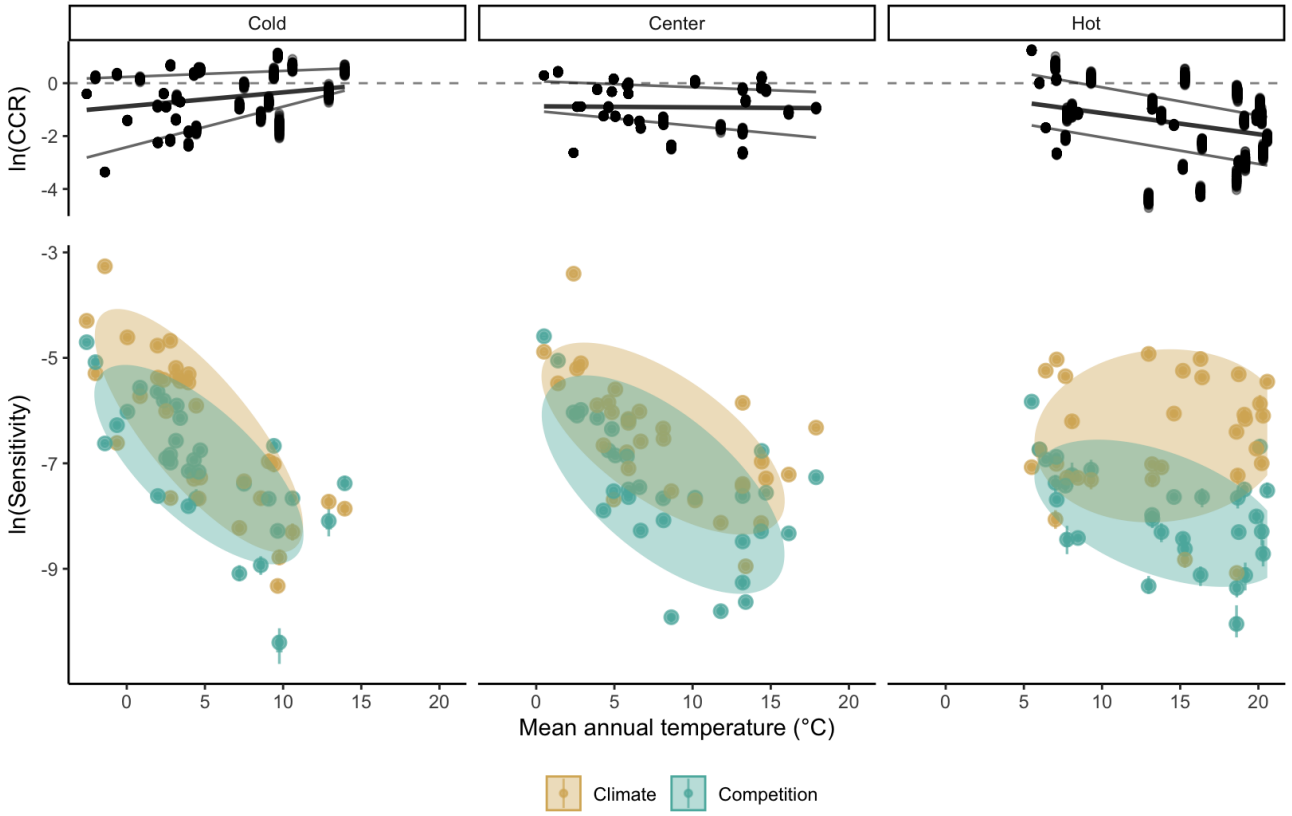

Figure 5: Bottom panels describe the sensitivity of species population growth rate to competition (green) and climate (yellow) across the cold, center, and hot temperature ranges. The top panels show the log ratio between competition and climate sensitivities, where negative values mean climate sensitivity is relatively higher than competition. We defined each species' temperature range position as the median Mean Annual Temperature across all observed plots for each cold, center, and hot range class. In the bottom panel, species points are grouped by a Multivariate Normal Density function with 75% probability, while in the top panel, the lines represent the 25, 50, and 75% quantile probabilities.

4 Discussion

We developed an integral projection model for 31 tree species linking growth, survival, and recruitment to stand level λ in order to assess the sensitivity of λ to climate and competition. Our model advances previous analysis of tree species performance by (i) explicitly incorporating climate and competition effects in the recruitment model, (ii) distinguishing between conspecific and heterospecific competition,

while (iii) tracking model's uncertainty at both the individual and plot levels. Moreover, we designed a modular approach that is easily extendable to include any of the over 200 available species in the dataset and additional covariates influencing each demographic rate.

The results reveal that, for all species, adding climate and competition covariates enhances the predictability of all demographic components in comparison to a simple random effect model without covariates. Nevertheless, the most influential variable remained the local plot conditions captured by the random effects. Therefore, we evaluated species sensitivity to climate and competition while considering plot-level variability. Across the species and their respective ranges, we found that λ was more sensitive to temperature and conspecific basal area of larger individuals. Furthermore, these sensitivities were contingent on the range position of the species, with climate being relatively more important than competition at both the cold and hot range border. These findings contribute to a better understanding of how tree species might respond to novel conditions arising from climate change and perturbations, providing valuable insights for their management.

Fit of demographic components

Our model demonstrated remarkable coherence when reproducing the known variation in traits related to growth, survival, and recruitment components found in the literature. The intercepts for growth and survival were correlated with maximal size and longevity (Burns et al. 1990), while the recruitment intercept aligned well with the seed mass (Díaz et al. 2022). Additionally, the models effectively reproduced the fast-slow continuum (Salguero-Gómez et al. 2016), showing a negative correlation between growth and survival rate and a positive correlation between growth and recruitment rate (Figure S14). Regarding competition, the model captured the negative correlation between density dependence and shade tolerance. The model also matches a common expectation of communities where species coexist, with a stronger response to conspecific competition relative to heterospecific competition, crucial for biodiversity maintenance (Chesson 2000). The intensity of conspecific density dependence was also higher for fast-growing trees than for slow-growing ones (Figure S15), similar to observations in tropical trees (Zhu et al. 2018). For climate, validation is challenging due to limited data on optimal temperature and precipitation measures. Nevertheless, our results align with others, indicating the presence of demographic compensation across forest trees (Bohner and Diez 2020, Yang et al. 2022).

Furthermore, the estimated breadth of response to climate correlates with the range size (Figure S16), suggesting that the model captures information not explicitly included.

Most of the variability in λ was associated with local plot conditions captured by random effects, akin to previous studies (Vanderwel et al. 2016, Le Squin et al. 2021). This implies the influence of other determinants of demography beyond climate and competition. For instance, at a local scale, soil nitrogen content (Ibáñez et al. 2018) and mixed mycorrhizal associations (Luo et al. 2023) can enhance growth rates. At larger scales, events such as wildfires and insect outbreaks play crucial roles in forest dynamics and stand structure (Franklin et al. 2002), causing synchronized mortality and altering stand composition and abundance. While we focused on quantifying the effect of climate and competition, other covariates may have greater importance in driving variance in demographic rates. For instance, tree growth models showed improved estimates when accounting for extreme climatic events (Sanginés de Cárcer et al. 2017), and unusual drought events, rather than average precipitation, were the highest predictors of tree fecundity after temperature (Clark et al. 2011).

λ *sensitivity to climate and competition*

We found that the sensitivity of λ was higher for temperature, followed by conspecific competition, across the species. Studies examining the relative impacts of climate and competition on tree performance yield diverse outcomes. For instance, while some suggest that competition has a higher effect on growth than climate (Gómez-Aparicio et al. 2011, Le Squin et al. 2021), others find the opposite (Copenhaver-Parry and Cannon 2016). Furthermore, the relative effect between climate and competition can change between demographic components, where growth is more sensitive to competition while fecundity to climate (Clark et al. 2011). This disparity may arise from a tendency to evaluate sensitivity to specific demographic rates rather than considering their integrated effects. This is particularly critical since the population growth rate does not respond equally to all covariates. We performed additional sensitivity analyses, which revealed that most species are primarily sensitive to recruitment, followed by survival, with a relatively lower impact from growth (see Supplementary Material 3).

Assessing climate sensitivity across the species range distribution revealed divergent responses. As species' performance changes nonlinearly with climate, lower sensitivity values to a climate covariate indicate that the species operates under optimal climate conditions, whereas higher sensitivity values

suggest the species is deviating from its optimal climate condition. Overall, climate sensitivity (primarily driven by MAT) was higher at both the cold and hot range extremes. This implies that species coming from colder temperatures exhibit optimal performance towards their warmer range, and vice versa for species from hotter conditions. Interestingly, the demographic components driving higher sensitivity to climate at the cold and hot extremes differ. The recruitment and growth models primarily influenced sensitivity at the cold border, while the survival model dominated at the hot border (see Figure S17). Previous studies have indicated climate-constrained growth rates at the cold border for North American (Ettinger and HilleRisLambers 2013) and European (Kunstler et al. 2021) trees. Consistent with our results, a decrease in survival at the hot border was observed for European trees (Kunstler et al. 2021), though not in eastern North America (Purves 2009).

The sensitivity of λ to competition increased almost linearly toward colder temperatures for most species. Due to the nonlinearity between species' performance and competition, the sensitivity of λ to changes in competition decreases as stand density increases (negative exponential shape). This implies that the observed decrease in sensitivity to competition toward the hot range results from an overall increase in stand density (i.e. competition intensity). Indeed, biotic interactions are often more critical at the warm range border (Paquette and Hargreaves 2021). However, when evaluating only the growth rate of North American (Ettinger and HilleRisLambers 2013) and European (Kunstler et al. 2011) trees, the effect of competition remains constant across the climate range.

Limitations and Future Perspectives

Structured population models, such as the IPM, play a crucial role in capturing ontogenetic variability within tree population dynamics. While the growth model inherently considers individual size, the survival and recruitment models are size-independent. We attempted to incorporate the widely assumed "U-shape" form of mortality rate changes with individual size (Lines et al. 2010), but it performed worse than the simple random effects one (Figure S6). Mortality has been observed to increase with individual size (Luo and Chen 2011, Hember et al. 2017), but its significance appears to manifest only when interacting with climate and competition (Le Squin et al. 2021). The challenge in capturing size dependence in the survival model likely stems from the lack of information on small individuals (dbh $<$ 12.7 cm) and the rarity of larger individuals in datasets, even for extensive forest inventories

(Canham and Murphy 2017). Despite not explicitly including individual size in the survival model, its indirect influence is included with the asymmetric competition, where smaller individuals experience higher competitive pressure. Another limitation of this model, shared with many models using forest inventory data (Kunstler2021; Le Squin et al. 2021, Guyennon et al. 2023), is its focus on adults, while tree fecundity can be influenced by climate (Clark et al. 2021), and the dynamics of recruitment may not necessarily align with those of adults (Serra-Diaz et al. 2016, Wason and Dovciak 2017, but see Canham and Murphy 2016).

The modular nature of our approach makes it easily extensible to include new species or covariates. For instance, additional covariates such as water balance or evapotranspiration could be tested to evaluate the impact of drought-induced mortality (Peng et al. 2011). Furthermore, exploring the interaction between climate, competition, and individual size can enhance predictions of demographic rates (Peng et al. 2011, Rollinson et al. 2016, Ford et al. 2017, Le Squin et al. 2021). An overlooked but computationally expensive improvement involves jointly fitting the growth, survival, and recruitment models. This would enable leveraging ecological knowledge, such as life history tradeoffs, by sharing information between processes with abundant data (e.g. growth) and those with scarce data (e.g. recruitment). Future steps should focus on better understanding the variability captured by random effects and translating it into ecological processes. While we addressed individual and plot-level model uncertainty, further considerations for other sources of variability arising from temporal stochasticity in climate and competition covariates are essential. This will enhance our understanding of the effects of spatiotemporal variability on species performance across their range (Holt et al. 2022).

References

Bohner, T., and J. Diez. 2020. Extensive mismatches between species distributions and performance and their relationship to functional traits. Ecology Letters 23:33–44.

Boucher-Lalonde, V., A. Morin, and D. J. Currie. 2012. How are tree species distributed in climatic space? A simple and general pattern. Global Ecology and Biogeography 21:1157–1166.

Briscoe, N. J., J. Elith, R. Salguero-Gómez, J. J. Lahoz-Monfort, J. S. Camac, K. M. Giljohann, M.

H. Holden, B. A. Hradsky, M. R. Kearney, S. M. McMahon, B. L. Phillips, T. J. Regan, J. R. Rhodes, P. A. Vesk, B. A. Wintle, J. D. L. Yen, and G. Guillera-Arroita. 2019. Forecasting species range dynamics with process-explicit models: matching methods to applications. Ecology Letters 22:1940–1956.

Burns, R. M., B. H. Honkala, and Others. 1990. Silvics of North America: 1. Conifers; 2. Hardwoods Agriculture Handbook 654. US Department of Agriculture, Forest Service, Washington, DC.

Canham, C. D., and L. Murphy. 2016. The demography of tree species response to climate: Seedling recruitment and survival. Ecosphere 7:1–16.

Canham, C. D., and L. Murphy. 2017. The demography of tree species response to climate: Sapling and canopy tree survival. Ecosphere 8.

Caswell, H. 2000. Matrix population models. Sinauer Sunderland, MA.

Chesson, P. 2000. Mechanisms of maintenance of species diversity. Annu. Rev. Ecol. Syst 31:343–66.

Clark, J. S., R. Andrus, M. Aubry-Kientz, Y. Bergeron, M. Bogdziewicz, D. C. Bragg, D. Brockway, N. L. Cleavitt, S. Cohen, B. Courbaud, R. Daley, A. J. Das, M. Dietze, T. J. Fahey, I. Fer, J. F. Franklin, C. A. Gehring, G. S. Gilbert, C. H. Greenberg, Q. Guo, J. HilleRisLambers, I. Ibanez, J. Johnstone, C. L. Kilner, J. Knops, W. D. Koenig, G. Kunstler, J. M. LaMontagne, K. L. Legg, J. Luongo, J. A. Lutz, D. Macias, E. J. B. McIntire, Y. Messaoud, C. M. Moore, E. Moran, J. A. Myers, O. B. Myers, C. Nunez, R. Parmenter, S. Pearse, S. Pearson, R. Poulton-Kamakura, E. Ready, M. D. Redmond, C. D. Reid, K. C. Rodman, C. L. Scher, W. H. Schlesinger, A. M. Schwantes, E. Shanahan, S. Sharma, M. A. Steele, N. L. Stephenson, S. Sutton, J. J. Swenson, M. Swift, T. T. Veblen, A. V. Whipple, T. G. Whitham, A. P. Wion, K. Zhu, and R. Zlotin. 2021. Continent-wide tree fecundity driven by indirect climate effects. Nature Communications 12:1–11.

Clark, J. S., D. M. Bell, M. H. Hersh, and L. Nichols. 2011. Climate change vulnerability of forest biodiversity: Climate and competition tracking of demographic rates. Global Change Biology 17:1834–1849.

Copenhaver-Parry, P. E., and E. Cannon. 2016. The relative influences of climate and competition on tree growth along montane ecotones in the Rocky Mountains. Oecologia 182:13–25.

Csergő, A. M., R. Salguero-Gómez, O. Broennimann, S. R. Coutts, A. Guisan, A. L. Angert, E. Welk, I. Stott, B. J. Enquist, B. McGill, J. C. Svenning, C. Violle, and Y. M. Buckley. 2017. Less favourable climates constrain demographic strategies in plants.

Díaz, S., J. Kattge, J. H. C. Cornelissen, I. J. Wright, S. Lavorel, S. Dray, B. Reu, M. Kleyer, C. Wirth, I. C. Prentice, and Others. 2022. The global spectrum of plant form and function: enhanced species-level trait dataset. Scientific Data 9:755.

Easterling, M. R., S. P. Ellner, and P. M. Dixon. 2000. Size-specific sensitivity: applying a new structured population model. Ecology 81:694–708.

Ellner, S. P., D. Z. Childs, and M. Rees. 2016. Data-driven modelling of structured populations. Springer.

Ettinger, A. K., and J. HilleRisLambers. 2013. Climate isn't everything: Competitive interactions and variation by life stage will also affect range shifts in a warming world. American Journal of Botany 100:1344–1355.

Evans, M. E. K., C. Merow, S. Record, S. M. McMahon, and B. J. Enquist. 2016. Towards Process-based Range Modeling of Many Species. Trends in Ecology and Evolution 31:860–871.

Ford, K. R., I. K. Breckheimer, J. F. Franklin, J. A. Freund, S. J. Kroiss, A. J. Larson, E. J. Theobald, and J. HilleRisLambers. 2017. Competition alters tree growth responses to climate at individual and stand scales. Canadian Journal of Forest Research 47:53–62.

Franklin, J. F., T. A. Spies, R. V. Pelt, A. B. Carey, D. A. Thornburgh, D. R. Berg, D. B. Lindenmayer, M. E. Harmon, W. S. Keeton, D. C. Shaw, K. Bible, and J. Chen. 2002. Disturbances and structural development of natural forest ecosystems with silvicultural implications, using Douglas-fir forests as an example. Forest Ecology and Management 155:399–423.

Gabry, J., R. Češnovar, and A. Johnson. 2023. cmdstanr: R Interface to 'CmdStan'.

513 Gelman, A., B. Goodrich, J. Gabry, and A. Vehtari. 2019. R-squared for Bayesian Regression Models.
514 American Statistician 73:307–309.

515 Gómez-Aparicio, L., R. García-Valdés, P. Ruíz-Benito, and M. A. Zavala. 2011. Disentangling the
516 relative importance of climate, size and competition on tree growth in Iberian forests: Implications
517 for forest management under global change. Global Change Biology 17:2400–2414.

518 Guisan, A., and N. E. Zimmermann. 2000. Predictive habitat distribution models in ecology. Ecological
519 Modelling 135:147–186.

520 Guyennon, A., B. Reineking, R. Salguero-Gomez, J. Dahlgren, A. Lehtonen, S. Ratcliffe, P. Ruiz-Benito,
521 M. A. Zavala, and G. Kunstler. 2023. Beyond mean fitness: Demographic stochasticity and resilience
522 matter at tree species climatic edges. Global Ecology and Biogeography 32:573–585.

523 Hember, R. A., W. A. Kurz, and N. C. Coops. 2017. Relationships between individual-tree mortality
524 and water-balance variables indicate positive trends in water stress-induced tree mortality across
525 North America. Global Change Biology 23:1691–1710.

526 Holt, R. D. 2009. Bringing the Hutchinsonian niche into the 21st century: Ecological and evolutionary
527 perspectives. Proceedings of the National Academy of Sciences 106:19659–19665.

528 Holt, R. D., M. Barfield, and J. H. Peniston. 2022. Temporal variation may have diverse impacts on
529 range limits. Philosophical Transactions of the Royal Society B: Biological Sciences 377.

530 Hutchinson, G. E. 1957. Concluding remarks. Pages 415–427 *in* Cold spring harbor symposium on
531 quantitative biology.

532 Ibáñez, I., D. R. Zak, A. J. Burton, and K. S. Pregitzer. 2018. Anthropogenic nitrogen deposition
533 ameliorates the decline in tree growth caused by a drier climate. Ecology.

534 Kohyama, T. 1992. Size-structured multi-species model of rain forest trees. Functional Ecology:206–212.

535 Kunstler, G., C. H. Albert, B. Courbaud, S. Lavergne, W. Thuiller, G. Vieilledent, N. E. Zimmermann,
536 and D. A. Coomes. 2011. Effects of competition on tree radial-growth vary in importance but not

in intensity along climatic gradients. Journal of Ecology 99:300–312.

Kunstler, G., A. Guyennon, S. Ratcliffe, N. Rüger, P. Ruiz-Benito, D. Z. Childs, J. Dahlgren, A. Lehtonen, W. Thuiller, C. Wirth, M. A. Zavala, and R. Salguero-Gomez. 2021. Demographic performance of European tree species at their hot and cold climatic edges. Journal of Ecology 109:1041–1054.

Le Squin, A., I. Boulangeat, and D. Gravel. 2021. Climate-induced variation in the demography of 14 tree species is not sufficient to explain their distribution in eastern North America. Global Ecology and Biogeography 30:352–369.

Lines, E. R., D. A. Coomes, and D. W. Purves. 2010. Influences of forest structure, climate and species composition on tree mortality across the Eastern US. PLoS ONE 5.

Louthan, A. M., D. F. Doak, and A. L. Angert. 2015. Where and When do Species Interactions Set Range Limits? Trends in Ecology and Evolution 30:780–792.

Luo, S., R. P. Phillips, I. Jo, S. Fei, J. Liang, B. Schmid, and N. Eisenhauer. 2023. Higher productivity in forests with mixed mycorrhizal strategies. Nature Communications 14:1–10.

Luo, Y., and H. Y. H. Chen. 2011. Competition, species interaction and ageing control tree mortality in boreal forests. Journal of Ecology 99:1470–1480.

Maguire Jr, B. 1973. Niche response structure and the analytical potentials of its relationship to the habitat. The American Naturalist 107:213–246.

McGill, B. J. 2012. Trees are rarely most abundant where they grow best. Journal of Plant Ecology 5:46–51.

McKenney, D. W., M. F. Hutchinson, P. Papadopol, K. Lawrence, J. Pedlar, K. Campbell, E. Milewska, R. F. Hopkinson, D. Price, and T. Owen. 2011. Customized Spatial Climate Models for North America. Bulletin of the American Meteorological Society 92:1611–1622.

Merow, C., A. M. Latimer, A. M. Wilson, S. M. Mcmahon, A. G. Rebelo, and J. A. Silander. 2014.

561 On using integral projection models to generate demographically driven predictions of species'
562 distributions: Development and validation using sparse data. Ecography 37:1167–1183.

563 Midolo, G., C. Wellstein, and S. Faurby. 2021. Individual fitness is decoupled from coarse-scale
564 probability of occurrence in North American trees. Ecography 44:789–801.

565 Milner-Gulland, E. J., and K. Shea. 2017. Embracing uncertainty in applied ecology. Journal of Applied
566 Ecology.

567 Ministère des Ressources Naturelles. 2016. Norme d'inventaire ecoforestier: placettes-echantillons
568 temporaires. Direction des inventaires forestier, Ministère des Ressources naturelles,Québec.

569 O'Connell, M. B., E. B. LaPoint, J. A. Turner, T. Ridley, D. Boyer, A. Wilson, K. L. Waddell, and
570 B. L. Conkling. 2007. The forest inventory and analysis database: Database description and users
571 forest inventory and analysis program. US Department of Agriculture, Forest Service.

572 Ohse, B., A. Compagnoni, C. E. Farrior, S. M. McMahon, R. Salguero-Gómez, N. Rüger, and T. M.
573 Knight. 2023. Demographic synthesis for global tree species conservation. Trends in Ecology and
574 Evolution 38:579–590.

575 Pacala, S. W., C. D. Canham, J. Saponara, J. A. Silander, R. K. Kobe, E. Ribbens, J. A. S. Jr., R.
576 K. Kobe, and E. Ribbens. 1996. Forest models defined by Field Measurements: Estimation, Error
577 Analysis and Dynamics. Ecological Monographs 66:1–43.

578 Pagel, J., and F. M. Schurr. 2012. Forecasting species ranges by statistical estimation of ecological
579 niches and spatial population dynamics. Global Ecology and Biogeography 21:293–304.

580 Paquette, A., and A. L. Hargreaves. 2021. Biotic interactions are more often important at species'
581 warm versus cool range edges. Ecology Letters 24:2427–2438.

582 Peng, C., Z. Ma, X. Lei, Q. Zhu, H. Chen, W. Wang, S. Liu, W. Li, X. Fang, and X. Zhou. 2011. A
583 drought-induced pervasive increase in tree mortality across Canada's boreal forests. Nature Climate
584 Change 1:467–471.

585 Pulliam, H. R. 2000. On the relationship between niche and distribution. Ecology Letters 3:349–361.

586 Purves, D. W. 2009. The demography of range boundaries versus range cores in eastern US tree species.
587 Proceedings of the Royal Society B: Biological Sciences 276:1477–1484.

588 Reich, P. B., M. G. Tjoelker, M. B. Walters, D. W. Vanderklein, and C. Buschena. 1998. Close
589 association of RGR, leaf and root morphology, seed mass and shade tolerance in seedlings of nine
590 boreal tree species grown in high and low light. Functional Ecology 12:327–338.

591 Rollinson, C. R., M. W. Kaye, and C. D. Canham. 2016. Interspecific variation in growth responses to
592 climate and competition of five eastern tree species. Ecology 97:1003–1011.

593 Russell, B. D., C. D. G. Harley, T. Wernberg, N. Mieszkowska, S. Widdicombe, J. M. Hall-Spencer, and
594 S. D. Connell. 2012. Predicting ecosystem shifts requires new approaches that integrate the effects
595 of climate change across entire systems. Biology Letters 8:164–166.

596 Salguero-Gómez, R., O. R. Jones, E. Jongejans, S. P. Blomberg, D. J. Hodgson, C. Mbeau-Ache, P. A.
597 Zuidema, H. De Kroon, and Y. M. Buckley. 2016. Fast–slow continuum and reproductive strategies
598 structure plant life-history variation worldwide. Proceedings of the National Academy of Sciences
599 113:230–235.

600 Sanginés de Cárcer, P., Y. Vitasse, J. Peñuelas, V. E. J. Jassey, A. Buttler, and C. Signarbieux. 2017.
601 Vapor-pressure deficit and extreme climatic variables limit tree growth. Global Change Biology
602 12:3218–3221.

603 Scherrer, D., Y. Vitasse, A. Guisan, T. Wohlgemuth, and H. Lischke. 2020. Competition and demography
604 rather than dispersal limitation slow down upward shifts of trees' upper elevation limits in the Alps.
605 Journal of Ecology:1–15.

606 Serra-Diaz, J. M., J. Franklin, W. W. Dillon, A. D. Syphard, F. W. Davis, and R. K. Meentemeyer.
607 2016. California forests show early indications of both range shifts and local persistence under
608 climate change. Global Ecology and Biogeography 25:164–175.

609 Sittaro, F., A. Paquette, C. Messier, and C. A. Nock. 2017. Tree range expansion in eastern North

America fails to keep pace with climate warming at northern range limits. Global Change Biology:1–10.

Svenning, J.-C. C., D. Gravel, R. D. Holt, F. M. Schurr, W. Thuiller, T. Münkemüller, K. H. Schiffers, S. Dullinger, T. C. Edwards, T. Hickler, S. I. Higgins, J. E. M. S. Nabel, J. Pagel, and S. Normand. 2014. The influence of interspecific interactions on species range expansion rates. Ecography 37:1198–1209.

Talluto, M. V., I. Boulangeat, S. Vissault, W. Thuiller, and D. Gravel. 2017. Extinction debt and colonization credit delay range shifts of eastern North American trees. Nature Ecology & Evolution 1:0182.

Team, S. D., and Others. 2022. Stan modeling language users guide and reference manual, version 2.30.1. Stan Development Team.

Thomas, C. D., A. Cameron, R. E. Green, M. Bakkenes, L. J. Beaumont, Y. C. Collingham, B. F. N. Erasmus, M. F. De Siqueira, A. Grainger, L. Hannah, and Others. 2004. Extinction risk from climate change. Nature 427:145–148.

Thuiller, W., T. Munkemuller, K. H. Schiffers, D. Georges, S. Dullinger, V. M. Eckhart, T. C. Edwards, D. Gravel, G. Kunstler, C. Merow, K. Moore, C. Piedallu, S. Vissault, N. E. Zimmermann, D. Zurell, F. M. Schurr, T. Münkemüller, K. H. Schiffers, D. Georges, S. Dullinger, V. M. Eckhart, T. C. Edwards, D. Gravel, G. Kunstler, C. Merow, K. Moore, C. Piedallu, S. Vissault, N. E. Zimmermann, D. Zurell, and F. M. Schurr. 2014. Does probability of occurrence relate to population dynamics? Ecography 37:1155–1166.

Tredennick, A. T., G. Hooker, S. P. Ellner, and P. B. Adler. 2021. A practical guide to selecting models for exploration, inference, and prediction in ecology. Ecology 102:e03336.

Vanderwel, M. C., H. Zeng, J. P. Caspersen, G. Kunstler, and J. W. Lichstein. 2016. Demographic controls of aboveground forest biomass across North America. Ecology Letters 19:414–423.

Villellas, J., D. F. Doak, M. B. García, and W. F. Morris. 2015. Demographic compensation among populations: What is it, how does it arise and what are its implications? Ecology Letters 18:1139–

1152.

Von Bertalanffy, L. 1957. Quantitative laws in metabolism and growth. The quarterly review of biology 32:217–231.

Wason, J. W., and M. Dovciak. 2017. Tree demography suggests multiple directions and drivers for species range shifts in mountains of Northeastern United States. Global Change Biology 23:3335–3347.

Yang, X., A. L. Angert, P. A. Zuidema, F. He, S. Huang, S. Li, S. L. Li, N. I. Chardon, and J. Zhang. 2022. The role of demographic compensation in stabilising marginal tree populations in North America. Ecology Letters 25:1676–1689.

Zhang, J., S. Huang, and F. He. 2015. Half-century evidence from western Canada shows forest dynamics are primarily driven by competition followed by climate. Proceedings of the National Academy of Sciences 112:4009–4014.

Zhu, K., C. W. Woodall, and J. S. Clark. 2012. Failure to migrate: Lack of tree range expansion in response to climate change. Global Change Biology 18:1042–1052.

Zhu, Y., S. A. Queenborough, R. Condit, S. P. Hubbell, K. P. Ma, and L. S. Comita. 2018. Density-dependent survival varies with species life-history strategy in a tropical forest. Ecology Letters.

Zuidema, P. A., E. Jongejans, P. D. Chien, H. J. During, and F. Schieving. 2010. Integral projection models for trees: a new parameterization method and a validation of model output. Journal of Ecology 98:345–355.